Dyes and Pigments 86 (2010) 233–237

Contents lists available at ScienceDirect

Dyes and Pigments

journal homepage: www.elsevier.com/locate/dyepig

High-efficiency undoped blue organic light-emitting device

Qing-Xiao Tong [a,b,*], Mei-Yee Chan [c], Shiu-Lun Lai [b,d], Tsz-Wai Ng [b,d], Peng-Fei Wang [e], Chun-Sing Lee [b,d], Shuit-Tong Lee [b,d,**]

[a] Department of Chemistry, Shantou University, Guangdong 515063, China
[b] Center of Super-Diamond and Advanced Films (COSDAF), City University of Hong Kong, Hong Kong SAR, China
[c] Department of Chemistry, The University of Hong Kong, Pokfulam Road, Hong Kong SAR, China
[d] Department of Physics and Materials Science, City University of Hong Kong, Hong Kong SAR, China
[e] Technical Institute of Physics and Chemistry, Chinese Academy of Sciences, Beijing 100080, China

ARTICLE INFO

Article history:
Received 10 December 2009
Received in revised form
20 January 2010
Accepted 21 January 2010
Available online 28 January 2010

Keywords:
High-efficiency
Non-doped
Blue
Organic light-emitting diode
Electroluminescence
Small-molecule

ABSTRACT

A high-efficiency, undoped, blue, organic light-emitting device was devised that employed a novel electroluminescent material 4-(7,10-diphenylfluoranthen-8-yl)-*N*,*N*-diphenylbenzenamine as electrofluorescence emitter. The device with a simple structure of ITO/*N*,*N*′-bis(1-naphthyl)-*N*,*N*′-diphenyl-1,1′-biphenyl-4,4′-diamine/4-(7,10-diphenylfluoranthen-8-yl)-*N*,*N*-diphenylbenzenamine/4,7-diphenyl-1,10-phenanthroline/LiF/Al exhibited stable blue light emission of CIE chromaticity coordinates ($x = 0.19 \pm 0.01$ and $y = 0.45 \pm 0.02$), and a current efficiency of 6.0 cd A^{-1} and a power efficiency of 4.6 lm W^{-1}.

1. Introduction

Since Tang and VanSlyke [1] first introduced efficient organic light-emitting devices (OLEDs), organic electroluminescent devices have attracted much scientific and commercial interest owing to their promising application in full-colour displays as well as large-area, flexible, lightweight light sources [2,3]. Full-colour displays require blue, green, and red emission elements with high device stability, high luminous efficiency and colour purity. Although significant improvement in OLED performance has been achieved over the past decades, further improvement is still required, especially in terms of the performance of blue OLEDs in the context of current efficiency and external quantum efficiency, which are relatively poor compared with red and green OLEDs. Blue-emitting materials are of interest not only as a major constituent of red–green–blue full-colour displays, but also as the key emitting element for generating white light in combination with the complementary yellow colour.

To improve electroluminescence (EL) quantum efficiency, doping of fluorescent or phosphorescent dyes in the emissive layer (EML) is the most effective approach adopted nowadays. However, the success of this doping method relies on the precise control of the small dopant amounts used, which are of the order ~0.1% [2,4]. This imposes pronounced manufacturing process control which increases production costs. In addition, phase separation in a guest-host system is also a potential problem [5–7]; recent investigation has proven that phase separation upon heating is an important cause of performance degradation in some guest-host system-based devices. Although host and guest molecules are initially homogeneously mixed, guest molecules commonly aggregate leading to phase separation during operation and/or upon heating [5–7]. Phase separation increases the host-guest distance beyond the capture radius R (1–10 nm) of a guest molecule for efficient host-guest energy transfer, thus rendering energy transfer ineffective [8]. This phenomenon can further reduce device lifetime, especially under high-temperature operation. In view of these shortcomings, considerable efforts have recently been devoted to the synthesis of high-efficiency non-doped blue-emitting materials [9–23].

Indeed, the molecular design of the structure of blue-emitting materials can influence their performance and thermal stability.

* Corresponding author. Tel.: +86 754 8290 2772; fax: +86 754 8290 2767.
** Corresponding author. Tel.: +86 852 2788 9606; fax: +86 852 2784 4696.
E-mail addresses: qxtong@gmail.com (Q.-X. Tong), apannale@cityu.edu.hk (S.-T. Lee).

0143-7208/$ – see front matter © 2010 Elsevier Ltd. All rights reserved.
doi:10.1016/j.dyepig.2010.01.009

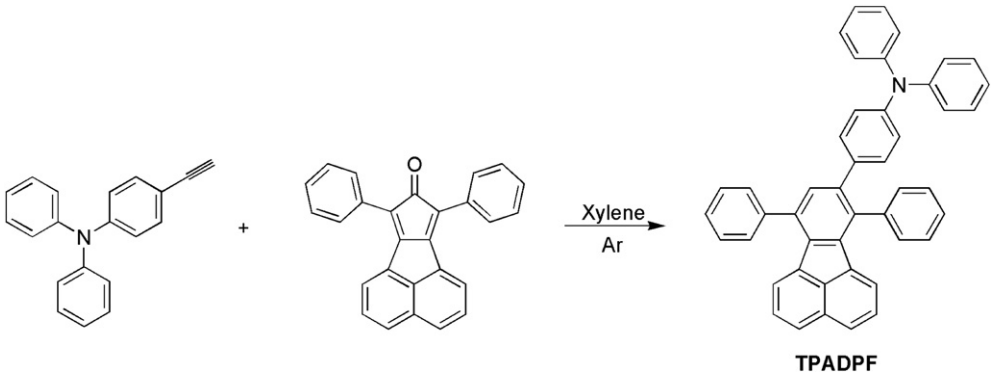

Scheme 1. Synthetic route of TPADPF.

Spiro-fluororene has received much attention as blue emitters because of its outstanding luminescent properties [24–26], although the multiple-step synthesis, coupled with low yields, are not commercially attractive. Chiechi et al. [9] recently developed a robust, fluoranthene derivative, fluorophore 7,8,10-triphenyl-fluoranthene (TPF), as a blue-emitting material in OLEDs. This compound was simply obtained in two synthetic steps from commercial starting materials and exhibited high quantum yield (0.86) in the solid-state. In addition, TPF can be employed as a single layer for light emission, in which the undoped device displayed maximum current and power efficiencies of 3.02 cd A^{-1} and 1.1 lm W^{-1}, respectively.

This paper concerns the synthesis and characterization of the fluoranthene derivative, 4-(7,10-diphenylfluoranthen-8-yl)-*N*,*N*-diphenylbenzenamine (TPADPF) which is obtained by a four step synthesis in high yield according to the Diels–Alder reaction. Comparing with unsubstituted TPF [9], diphenylamine was introduced at carbon 4 position of the benzene ring 8 because of its rigid structure and hole transporting properties that are important for producing an undoped emitting material.

2. Experimental

2.1. Material synthesis

The fluoranthene derivative TPADPF was synthesized according to the Diels–Alder reaction [9,27,28] (Scheme 1). 4-ethynyl-*N*,*N*-diphenylbenzene amine [28] and 7,9-diphenyl-8H-cyclopenta[l] acenaphthylen-8-one [29] were synthesized according to literature procedures. All solvents were purified by routine procedures.

2.2. Synthesis of TPADPF

4-ethynyl-*N*,*N*-diphenylbenzene amine (807 mg, 3.0 mmol) and 7,9-diphenyl-8H-cyclopenta[l]acenaphthylen-8-one (1.07 g, 3.0 mmol) were dissolved in *o*-xylene (40 mL) under an argon atmosphere and the resultant mixture was heated for 24 h at 170 °C (oil bath temperature). After the mixture was cooled to room temperature, ethanol (200 mL) was added. The precipitate was filtered, washed with ethanol (300 mL) and dried in a vacuum, followed by column chromatography (dichloromethane/petroleum ether, 1:6) on silica gel, TPADPF was obtained as a slightly yellow and strongly fluorescent solid. Yield: 85%. ^{1}H NMR (CD_2Cl_2, 400 MHz): δ 7.78–7.68 (m, 4H), 7.61–7.52 (m, 3H), 7.48–7.18 (m, 12H), 7.12–6.95 (m, 9H), 7.14 (d, $J = 7.2$, 2H), 6.74 (d, $J = 7.2$, 1H),. MS: m/z 597. Anal. Calcd for $C_{46}H_{31}N$: C, 92.43; H, 5.23; N, 2.34. Found: C, 94.55; H, 5.28; N, 2.28.

2.3. Device fabrication and characterization

Fig. 1 shows the structures of *N*,*N*′-bis(1-naphthyl)-*N*,*N*′-diphenyl-1,1′-biphenyl-4,4′-diamine (NPB) and 4,7-diphenyl-1,10-phenanthroline (BPhen). Devices were constructed on a glass substrate which had been pre-coated with a patterned layer of indium-tin oxide (ITO) having a sheet resistance of 30 Ω square^{-1}. Substrates were cleaned with isopropyl alcohol, *Decon 90*, and deionized water and then dried in an oven, before being finally treated in a UV-ozone chamber. All organic and metal layers were grown in succession without breaking vacuum (at a base pressure of 10^{-6} mbar). Deposition rates were monitored with a quartz oscillation crystal and controlled at 0.1–0.2 nm/s for both organic and metal layers. A shadow mask was used to define the cathode to make four 0.1 cm^2 devices on each substrate. EL spectra and current density-voltage-luminance (J-V-L) characteristics of OLEDs were measured with a programmable Keithley model 237 power source and a Spectrascan PR650 photometer under ambient condition. ^{1}H NMR spectra were recorded with a Bruker DPX-400 spectrometer (400 MHz). Mass spectrometry (MS) was performed on a PE SCIEX LC/MS spectrometer. Elemental analyses (EA) were performed on a Vario EL Elementar by the Flash EA 1112 method. Absorption and photoluminescence (PL) spectra of TPADPF were measured with

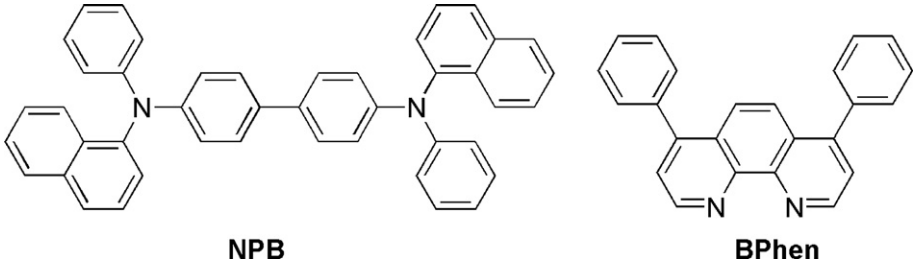

Fig. 1. Chemical structures of NPB and BPhen.

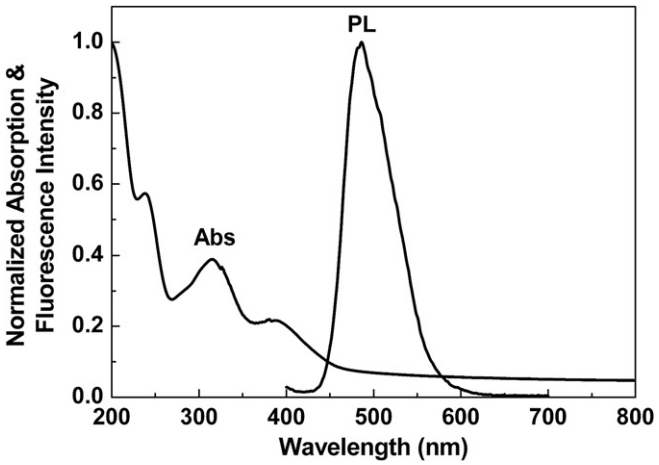

Fig. 2. Absorption and PL spectra of thermally evaporated thin film of TPADPF on a quartz substrate.

a Perkin Elmer Lambda 2S US/VIS spectrometer and a Perkin Elmer LS 50B luminescence spectrometer, respectively. The ionization potential (I_P) of TPADPF was measured with ultraviolet photoelectron spectroscopy (UPS) in a VG ESCALAB 220i-XL surface analysis system, whereas the electron affinity (E_A) was estimated by subtracting from the optical bandgap (E_g) determined by the absorption spectrum of its solid-state film.

3. Results and discussion

3.1. Photo-physical characteristics of TPADPF

TPADPF was synthesized in-house according to the synthesis route in Scheme 1, and its molecular structure was confirmed with mass spectrometry, ^{1}H nuclear magnetic resonance, and elemental analyses. Fig. 2 shows the absorption and PL spectra of vacuum-deposited thin film of TPADPF on a quartz substrate. It can be seen that the PL spectrum has a strong blue emission peak at 486 nm under direct excitation at 386 nm, while the absorption spectrum has its characteristic peaks at 385, 314, and 238 nm, respectively.

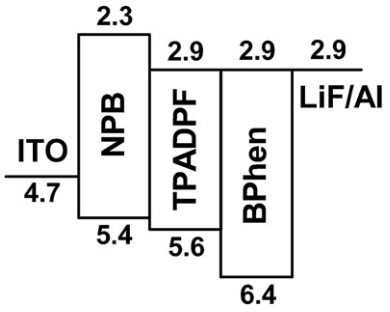

Fig. 4. Energy level diagram for the TPADPF-based device.

The E_g for TPADPF is 2.7 eV, calculated from the onset of the thin film absorption spectrum.

3.2. Electronic structure of TPADPF

UPS is the useful tool for obtaining the electronic band structures of organics. Some important values, for instance, I_P and the highest occupied states (HOS) can be obtained from UPS. Fig. 3 shows a He I ($h\nu = 21.22$ eV) UPS spectrum of the TPADPF film under ultra-high vacuum conditions. The inelastic electron cutoff and the HOS of the highest occupied molecular orbital (HOMO) are also enlarged. With reference to these values, I_P could be calculated by $I_P = 21.22 - (25.32 - 9.70) = 5.6$ eV. Subtracting the E_g of 2.7 eV from the I_P, the E_A of TPADPF was estimated to be 2.9 eV. Fig. 4 illustrates the energy level diagram for the TPADPF-based device.

3.3. Device characteristics of TPADPF

In order to investigate EL properties of organic TPADPF, OLEDs with architectures of: (A) ITO/TPADPF (100 nm)/BPhen (20 nm)/LiF (0.5 nm)/Al (100 nm); and (B) ITO/NPB (70 nm)/TPADPF (30 nm)/BPhen (20 nm)/LiF (0.5 nm)/Al (100 nm) were fabricated by thermal vapor deposition, whereas NPB and BPhen served as a hole transporting and an electron transporting materials, respectively, and TPADPF functioned as both hole transporting and light-emitting material. Fig. 5 shows the EL spectra for devices A

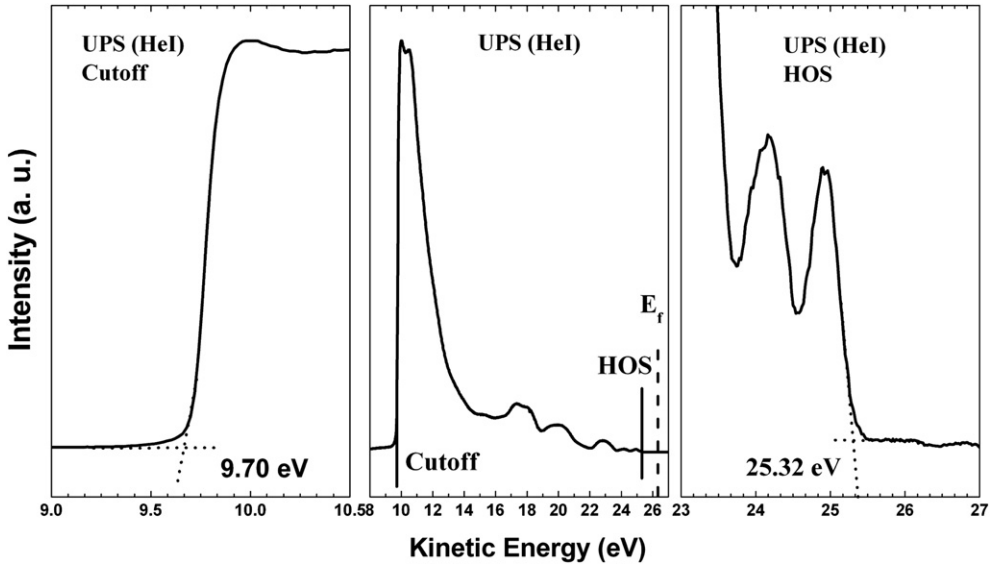

Fig. 3. UPS spectrum of a TPADPF film obtained with He I excitation.

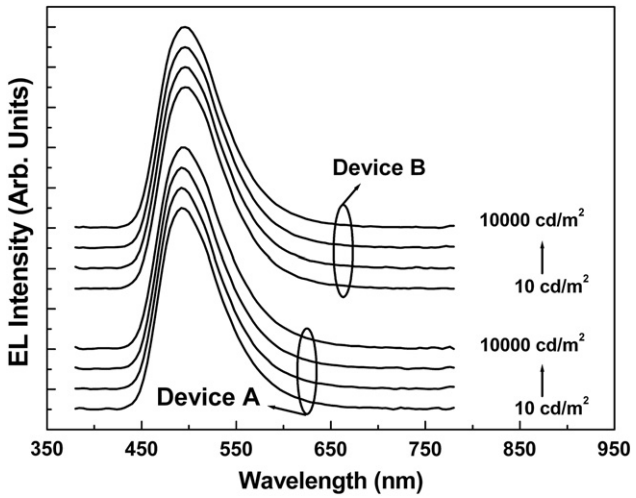

Fig. 5. EL spectra of device A and device B viewed in the normal direction at the luminescence of 10, 100, 1000, and 10,000 cd/m^2, respectively.

and B viewed in the normal direction at different luminance (L) levels. As seen in Fig. 5, both devices A and B exhibited blue light. The EL spectral peaks centered at 492 nm with the full spectral widths at half maxima (FWHM) of 73.5, 73.5, 74.3, and 77.9 nm for device A while the peaks located at 496 nm with FWHM of 76.3, 76.5, 76.8, and 77.0 nm for device B at the $L = 10$, 100, 1000, and 10,000 cd/m^2, respectively. The corresponding CIE 1931 chromaticity coordinates of ($x = 0.19 \pm 0.01$, $y = 0.43 \pm 0.02$) for device A and ($x = 0.19 \pm 0.01$, $y = 0.45 \pm 0.02$) for device B, respectively. It should be highlighted that our recent study on the use of another new blue emitter 4,4′,4″-trispyrenylphenylamine (TPyPA) showed exciplex formation at the TPyPA/BPhen contact as a consequence of an additional yellow emission peak at 570 nm [17]. On the contrary, exciplex formation does not occur in the present devices, which may be attributed to a weaker electron donating property of TPADPF as compared to TPyPA.

The electrical characteristics of devices A and B are depicted in Fig. 6. Under the same operating voltage, device B demonstrates a lower current density and a higher luminance than device A, even though the turn-on voltage (defined as voltage required to obtain a luminance of 1 cd/m^2) of both devices are the same ($V_{\text{turn-on}} = 2.6$ V). For instance, at the operating voltage of 5 V, the current density and the luminance for device A are 114.6 mA/cm^2 and

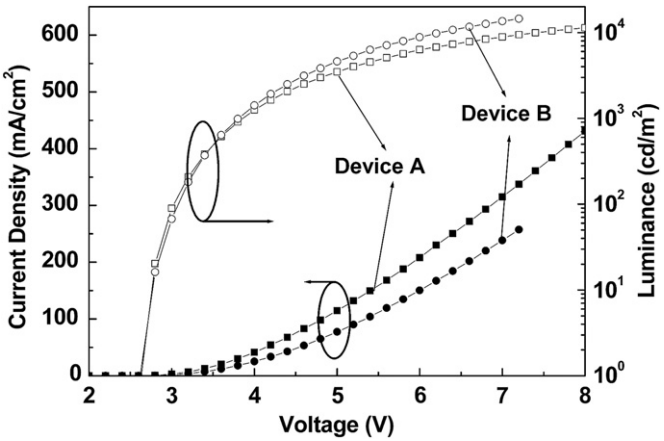

Fig. 6. J-V-L characteristics of the TPADPF-based devices.

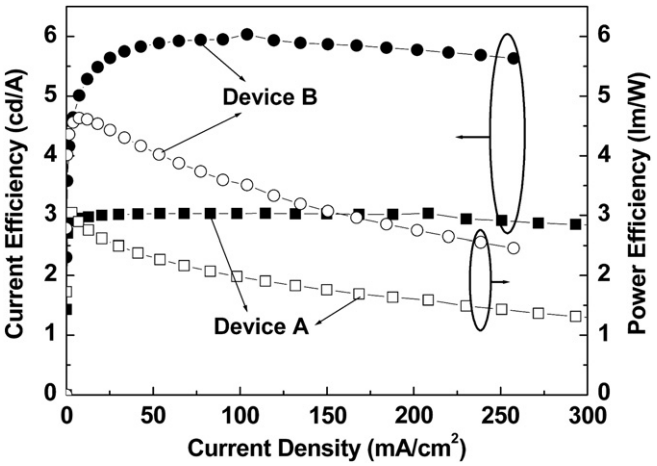

Fig. 7. Current efficiency-current density-power efficiency characteristics of the TPADPF-based devices.

3477 cd/m^2, respectively; whilst those for device B are only 77.4 mA/cm^2 and 4597 cd/m^2. Surprisingly, the driving voltage for device A is much lower than that for device B at the same current density. It is commonly realized that NPB can act as a stepping-stone to enhance hole injection from ITO to EML, resulting in a reduction of driving voltage. However, it is not the case for the present TPADPF-based devices. The reasons behind this phenomenon may be attributed to the elimination of current/luminescence quenching sites at the contact of ITO/TPADPF; particularly NPB with relatively small E_A ($\sim$2.3 eV) can function as an electron-blocking layer at the ITO/TPADPF interface. Another factor may be ascribed to different carrier mobilities in organic layers [30], in which the hole mobility in TPADPF is comparatively higher than that in NPB, thus resulting in a lower driving voltage.

Apart from the J-V-L characteristics, the incorporation of NPB can improve device efficiencies. As shown in Fig. 7, the maximum current and power efficiencies of device A are 3.0 cd/A ($\eta_{EQE} =$ 1.20%) and 3.1 lm/W, respectively, whereas those of device B are 6.0 cd/A ($\eta_{EQE} = 2.37\%$) and 4.6 lm/W, respectively (η_{EQE} is the external quantum efficiency). The performance improvement for device B can be assigned to be a better confinement of hole and electron currents within the TPADPF layer, which may be due to the lower hole mobility in NPB than that in TPADPF as well as the elimination of the quenching sites by incorporation of low E_A of NPB, consistent with the J-V-L characteristics. It is worth pointing out that the problematic roll-off characteristic of current efficiency at high operational brightness is not observed in the present devices. There is only a slight change in current efficiencies of 2.9 and 5.8 cd/A for devices A and B (only $\sim$3% drop from the maximum values) even at the current density as high as 250 mA/cm^2. Although its colour purity has room for improvement, these excellent device performance does show that TPADPF is the suitable candidate for commercial lighting/display applications.

4. Conclusions

In summary, we have fabricated a highly efficient non-doped blue OLED by using a novel EL material TPADPF. The device with a simple structure of ITO/NPB/TPADPF/BPhen/LiF/Al demonstrated a high current efficiency of 6.0 cd/A, and a high power efficiency of 4.6 lm/W. It shows stable blue emission with the CIE coordinates of ($x = 0.19 \pm 0.01$, $y = 0.45 \pm 0.02$), with the CIE coordinates and the FWHM remaining unchanged over a wide luminance range.

The present results demonstrate that TPADPF is a promising candidate as a blue-emitting material in OLEDs.

Acknowledgements

This work was supported by the Key Laboratory of Photochemical Conversion and Optoelectronic Materials,TIPC,CAS and Li Ka Shing Foundation.

References

[1] Tang CW, Van Slyke SA. Organic electroluminescent diodes. Appl Phys Lett 1987;51:913.
[2] Tang CW, Van Slyke SA, Chen CH. Electroluminescence of doped organic thin films. J Appl Phys 1989;65:3610.
[3] Chen CH, Shi J, Tang CW. Recent developments in molecular organic electroluminescent materials. Macromol Symp 1997;125:1.
[4] Lee MT, Chen HH, Liao CH, Tsai CH, Chen CH. Stable styrylamine-doped blue organic electroluminescent device based on 2-methyl-9,10-di(2-naphthyl) anthracene. Appl Phys Lett 2004;85:3301.
[5] Zhong GY, Xu Z, Zhang ST, Zhan YQ, Wang XJ, Xiong ZH, et al. Aggregation and permeation of 4-(dicyanomethylene)-2-methyl-6-(p-dimethylaminostyryl)-4H-pyran molecules in Alq. Appl Phys Lett 2002;81:1122.
[6] Chang SC, He G, Chen FC, Guo TF, Yang Y. Degradation mechanism of phosphorescent-dye-doped polymer light-emitting diodes. Appl Phys Lett 2001;79:2088.
[7] Gong JR, Wan LJ, Lei SB, Bai CL, Zhang XH, Lee ST. Direct evidence of molecular aggregation and degradation mechanism of organic light-emitting diodes under joule heating: an STM and photoluminescence study. J Phys Chem B 2005;109:1675.
[8] Baldo MA, O'Brien DF, You Y, Shoustikov A, Sibley S, Thompson ME, et al. Highly efficient phosphorescent emission from organic electroluminescent devices. Nature 1998;395:151.
[9] Chiechi RC, Tseng RJ, Marchioni F, Yang Y, Wudl F. Efficient blue-light-emitting electroluminescent devices with a robust fluorophore: 7,8,10-triphenylfluoranthene. Adv Mater 2006;18:325.
[10] Robinson MR, Bazan GC, O'Regan MB. Synthesis, morphology and optoelectronic properties of tris[(N-ethylcarbazolyl)(3,5-hexyloxybenzoyl)methane](phenanthroline)europium. Chem Commun 2000:1645.
[11] Murata H, Kafafi ZH, Uchida M. Efficient organic light-emitting diodes with undoped active layers based on silole derivatives. Appl Phys Lett 2002;80:189.
[12] Lee CL, Kang NG, Cho YS, Lee JS, Kim JJ. Polymer electrophosphorescent device: comparison of phosphorescent dye doped and coordinated systems. Opt Mater 2003;21:119.
[13] Xin H, Li FY, Guan M, Huang CH, Sun M, Wang KZ, et al. Carbazole-functionalized europium complex and its high-efficiency organic electroluminescent properties. J Appl Phys 2003;94:4729.
[14] Lo SC, Namdas EB, Burn PL, Samuel IDW. Synthesis and properties of highly efficient electroluminescent green phosphorescent iridium cored dendrimers. Macromolecules 2003;36:9721.
[15] Wong WY, He Z, So SK, Tong KL, Lin Z. A multifunctional platinum-based triplet emitter for OLED applications. Organometallics 2005;24:4079.
[16] Li Y, Rizzo A, Salerno M, Mazzeo M, Huo C, Wang Y, et al. Multifunctional platinum porphyrin dendrimers as emitters in undoped phosphorescent based light emitting devices. Appl Phys Lett 2006;89:061125.
[17] Tong QX, Lai SL, Chan MY, Tang JX, Kwong HL, Lee CS, et al. High-efficiency nondoped white organic light-emitting devices. Appl Phys Lett 2007;91:023503.
[18] Tong QX, Lai SL, Chan MY, Lai KH, Tang JX, Kwong HL, et al. Efficient green organic light-Emitting devices with a nondoped dual-functional electroluminescent material. Appl Phys Lett 2007;91:153504.
[19] Zhao L, Zou JH, Huang J, Li C, Zhang Y, Sun C, et al. Asymmetrically 9,10-disubstituted anthracenes as soluble and stable blue electroluminescent molecular glasses 2008;9:649.
[20] Huang J, Qiao X, Xia Y, Zhu X, Ma D, Cao Y, et al. A dithienylbenzothiadiazole pure red molecular emitter with electron transport and exciton self-confinement for nondoped organic red-light-emitting diodes. Adv Mater 2008;20:4172.
[21] Tong QX, Lai SL, Chan MY, Zhou YC, Kwong HL, Lee CS, et al. High-efficiency nondoped green organic light-emitting devices. Chem Phys Lett 2008;455:79.
[22] Tong QX, Lai SL, Chan MY, Zhou YC, Kwong HL, Lee CS, et al. Highly efficient blue organic light-Emitting device based on a nondoped electroluminescent material. Chem Mater 2008;20:6310.
[23] Tong QX, Lai SL, Chan MY, Zhou YC, Kwong HL, Lee CS, et al. A high performance nondoped blue organic light-Emitting device based on a diphenylfluoranthene-substituted fluorene derivative. J Phys Chem C 2009;113:6227.
[24] Katsis D, Geng YH, Ou JJ, Culligan SW, Trajkovska A, Chen SH, et al. Spiro-linked ter-, penta-, and heptafluorenes as novel amorphous materials for blue light emission. Chem Mater 2002;14:1332.
[25] Wong KT, Chien YY, Chen RT, Wang CF, Lin YT, Chiang HH, et al. Ter(9,9-diarylfluorene)s: highly efficient blue emitter with promising electrochemical and thermal stability. J Am Chem Soc 2002;124:11576.
[26] Wu CC, Liu TL, Hung WY, Lin YT, Wong KT, Chen RT, et al. Unusual nondispersive ambipolar carrier transport and high electron mobility in amorphous ter(9,9-diarylfluorene)s. J Am Chem Soc 2003;125:3710.
[27] Park YI, Lee SE, Park JW, Oh SY. New multi-phenylated carbazole derivatives for OLED through Diels-Alder reaction. Mol Cryst Liq Cryst 2007;470:223.
[28] Tong QX, Lai SL, Chan MY, Lai KH, Tang JX, Kwong HL, et al. High Tg triphenylamine-based starburst hole-transporting material for organic light-emitting devices. Chem Mater 2007;19:5851.
[29] Wehmeier M, Wagner M, Müllen K. Novel perylene chromophores obtained by a facile oxidative cyclodehydrogenation route. Chem Eur J 2001;7:2197.
[30] Xia ZY, Xiao X, Su JH, Chang CS, Chen CH, Li DL, et al. Low driving voltage and efficient orange-red phosphorescent organic light-emitting devices based on a benzotriazole iridium complex. Synthetic Metals 2009;159:1782.